

STRUCTURAL, OPTICAL AND FERROELECTRIC PROPERTIES OF BaTiO₃ CERAMICS

V. N. REDDY*, K. C. BABU NAIDU, T. SUBBARAO

Materials Research Lab, Dept. of Physics, S. K. University, Anantapur – 515 003, A. P, India

This investigation mainly deals with the structural, optical and ferroelectric properties of barium titanate (BT) ceramics synthesized via conventional solid state reaction method. The phase purity is evaluated from diffraction studies. The morphology is analyzed by scanning electron microscope. The diffuse reflectance spectrum (DRS) attributes the direct and indirect optical band gap energies of BT. In addition, IR spectrum confirms the presence of metal oxide (M-O) bonds such as Ti-O and Ba-O. The ferroelectric behavior (P-E loop) of BT as a function of temperature is also studied.

(Received May 10, 2016; Accepted July 5, 2016)

Keywords: Structure; Scanning Electron Microscopy; Optical Properties; Ferroelectric Properties

1. Introduction

Ceramic materials have potential applications due to their electrical properties [1]. In particular, the ceramic materials with ferroelectric properties have been developed and utilized for a variety of applications such as; non volatile memories, medical ultrasound imaging and actuators, and data storage devices [2]. The biggest applications of ferroelectric ceramics have been in the areas of dielectric ceramics for capacitor applications, especially ferroelectric thin film technology [3]. The perovskite family shows a structure of the type ABO₃ [4]. Many ferroelectric materials such as; barium titanate (BaTiO₃), lead titanate (PbTiO₃), lead zirconate titanate (PZT), lead lanthanum zirconate titanate (PLZT), have this perovskite type structure.

Usually, ferroelectric behavior is investigated with the help of P-E loop tracer. To the best of author's knowledge in the literature survey, there is no detailed report on polarization (P) versus electric field (E) variations as a function of temperature. Hence, an attempt has been made to elucidate the temperature dependence of ferroelectric properties such as saturated polarization (P_s), remanance polarization (P_r) and coercive field (E_c). In addition, the structural, morphological and optical properties are carried out.

2. Experimental Procedure

In this study the precursors are chosen as Ba(NO₃)₂ (99.6% purity, Sigma Aldrich), TiO₂ (99.4% purity, Sigma Aldrich) to prepare the ferroelectric barium titanate ceramics. Initially, the raw materials are weighed and mixed uniformly according to their stoichiometric ratio. The mixed powder is ball milled for approximately 12 hours in a ball miller (Retsch PM200). Furthermore, the uniformly grounded powder is presintered at 1000°C for 12 hr. The presintered powder is again ground for nearly 2 hr. The pellets of radius 0.59 cm and thickness 0.288 cm are prepared after applying 5 ton pressure using hydraulic press. The pellets are sintered at 1100°C for 2 hr in conventional furnaces. Further, the pellets are characterized using XRD at room temperature

* Corresponding author: vnr9490541633@gmail.com

(Bruker X-Ray Powder Diffract Meter, $\text{Cu}_{K\alpha} = 0.15418 \text{ nm}$), SEM (Hitachi: S-4700), EDAX (AMETEK system), JASCO UV-Visible spectrophotometer (V-670 PC), FT-IR spectrophotometer (IR affinity-1, Shimadzu) and P-E loop measurement (Marine India) for structural, surface morphological, elemental analysis, optical and ferroelectric properties respectively.

3. Results and Discussions

3.1 Structural Analysis

The diffraction pattern of BaTiO_3 ceramic powder is shown in Fig.1. It can be understood from figure that the formed single crystalline phases that belong to cubic perovskite structure of pure barium titanate. These phases are in consistent with standard JCPDS file No: 89-2475. These phases are indexed with miller indices (hkl) and compared with standard JCPDS data as depicted in Fig.1. The maximum intensity of 1466 is recorded for (110) plane at a two-theta angle of 31.787° . This peak attributes lattice parameter (a) of 3.972 \AA for the present material which is almost in close agreement with JCPDS: 89-2475. Furthermore, the average crystalline size (D) is calculated as 27.3 nm using the Scherer formula [5]. Also, the elastic strain ($\epsilon \sim 0.0028$) is evaluated from a standard relation mentioned reference [6]. The X-ray density (d_x) of $\sim 5.4268 \text{ g/cm}^3$ is obtained using a formula: ZM/Na^3 , where 'Z' is the no. of molecules per unit cell ($Z = 1$), 'M' is the molecular weight of the composition, 'N' is Avogadro's number (6.023×10^{23}) and 'a' is the lattice parameter. Further, the bulk density (d_b) is evaluated with the help of Archimedes principle [7]. The pore fraction of (P) is found to be ~ 0.121 by an equation: $P \sim 1 - (d_b/d_x)$ [4]. The smallest value of pore fraction establishes a fact that the present material may be of good dense.

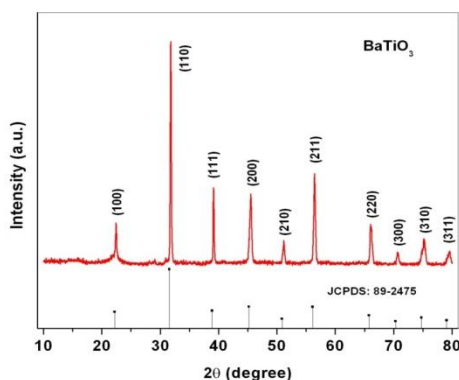


Fig.1 The diffraction pattern of BaTiO_3

Williamson-Hall (W-H) plot is shown in Fig.2. It is drawn for $\beta \cos\theta$ against $4\sin\theta$ for calculating micro-strain (ϵ') and crystallite size (D) from the equation: [8].

$$\beta \cos\theta = \frac{0.9\lambda}{D} + 4\epsilon' \sin\theta \quad (1)$$

where slope of straight line provides micro-strain while crystallite size is related to intercept part. This gives a relationship between ' ϵ' ' and 'D' values. The strain found from W-H plot is almost consistent with elastic strain (ϵ). In addition, the crystallite size $\sim 32.4 \text{ nm}$ (from W-H plot) is comparable to Scherer size.

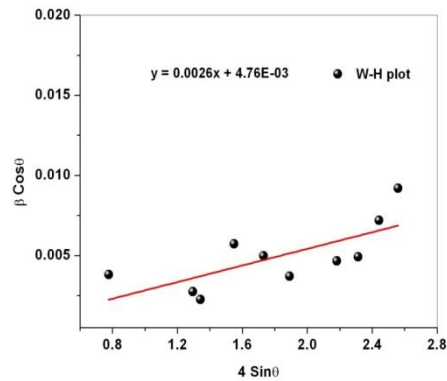


Fig.2 The W-H plot of $BaTiO_3$

3.2 SEM and EDS

The Scanning Electron Microscope (SEM) provides the surface morphology of powder specimen. It is seen from Fig. 3 that all the grains are of almost spherical in shape. The average grain size (G_a) is found to be 894 nm using linear intercept method [4].

$$G_a = 1.5L/MN \quad (2)$$

where L is the test line length, N is the number of intersecting grains and M is the magnification. EDS is generally used for finding the abundances of specific elements present in a material. EDS image (Fig.3) is shown along with the SEM image. It contains atomic and weight percentages of elements of Ba, Ti and O. This reveals the absence of impurities in the compound.

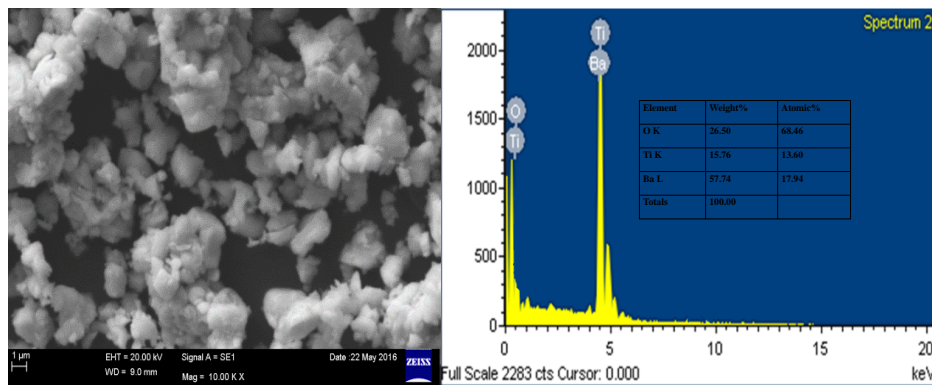


Fig.3 The SEM and EDS images of $BaTiO_3$

3.3 Optical Properties

3.3.1 UV-Visible Spectrum

The diffuse reflectance spectrum (DRS) is recorded in the range of 200-800 nm (Fig.4 (a)) for finding optical band gap energy of powder samples. Kubelka- Munk function of reflectance $F(r)$ is used to determine band gap [9].

$$F(r) = \frac{(1-r)^2}{2r} \quad (3)$$

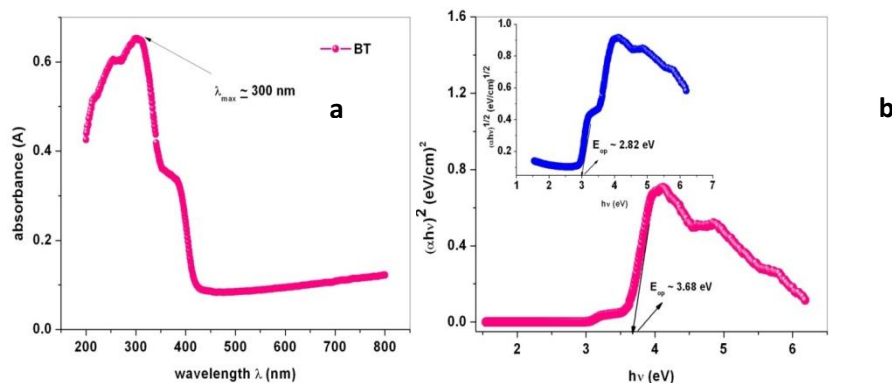


Fig.4 (a) The absorption spectrum and (b) $(\alpha hv)^2$ versus photon energy hv (eV) plot of $BaTiO_3$

The maximum absorption wavelength is recorded to be 300 nm. The absorption coefficient (α) is directly proportional to $F(r)$ and hence an equation to find band gap can be written as follows.

$$(\alpha hv)^n = m (hv - E_g) \quad (4)$$

Where m = Energy- independent constant that depends on transition probability, E_g = optical band gap energy, n = the kind of transition i.e. $n = 2$ for direct transition, $2/3$ for direct forbidden transition, $1/2$ for indirect transition, $1/3$ for indirect forbidden transition and hv = photon energy [10]. In this study direct and indirect transitions are considered. E_{op} value is evaluated from the linear portion that is extrapolated towards X-axis for $(\alpha hv)^2$ versus photon energy hv (eV) plot as α tends to zero (Fig.4 (b)). The optical band gap energies for direct and indirect transitions are calculated as 3.68 eV and 2.82 eV respectively.

FTIR Analysis

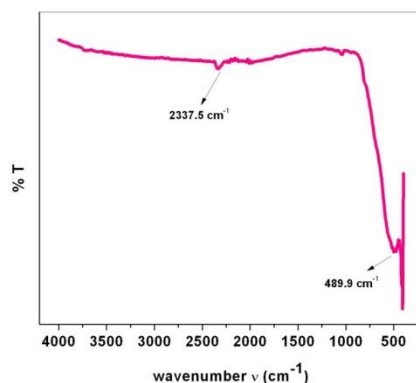


Fig.5 FTIR spectrum of $BaTiO_3$

Fourier Transform Infrared Spectroscopy (FTIR) spectrum is generally used for the determination of metal oxide bonds of ceramics. The FTIR spectrum of barium titanate ceramics sintered at 1100°C is recorded in the range of 400 - 4000 cm^{-1} (Fig. 5) and showed metal oxide ($Ba-O$ & $Ti-O$) absorption bands at 489.9 cm^{-1} and 2337.5 cm^{-1} [11].

3.4 Ferroelectric (P-E loop) Properties

The ferroelectric behavior of BT is investigated with the help of P-E loop tracer. While doing measurement the pellet is connected parallel to $4\mu\text{F}$ capacitor for compensation. Fig. 6 depicts the ferroelectric hysteresis loops of BT under an applied frequency of 600 Hz at an operating voltage of 600 V. It is understood from Fig. 6 that the sample shows a well-behaved hysteresis loop distorted into 'banana' shape performed at distinct temperatures such as 303K,

323K, 373K, 423K & 473K. This causes current leakage due to oxygen vacancies on the surface of the grains, instead of polarization. The response of dipoles per unit field is in general regarded as polarization. It is an observed fact that the saturation polarization (P_s) and remanance polarization (P_r) of BT at all temperatures is found to be constant value of $\approx 0.005 \mu\text{C}/\text{cm}^2$. It is observed that with increase of temperature the applied field required for saturation is slowly decreasing.

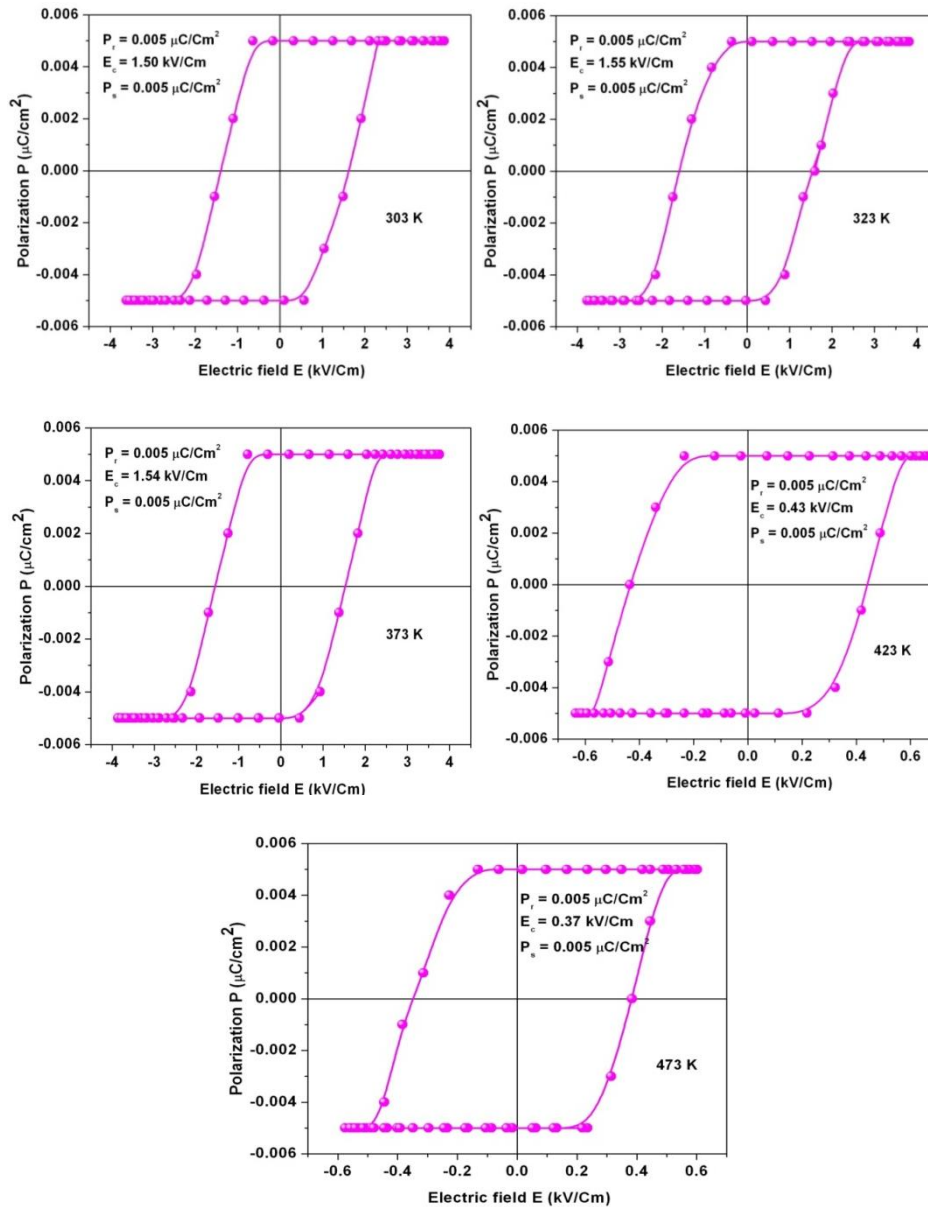


Fig.6 Temperature dependence of P-E loop behavior of BaTiO_3

The coercive electric field (E_c) as a function of temperature is shown in Fig. 7. Initially, E_c is noticed to be increasing temperature up to 373K and further it starts decreasing. It can be attributed to the Curie transition temperature that is normally occurs at 393K.

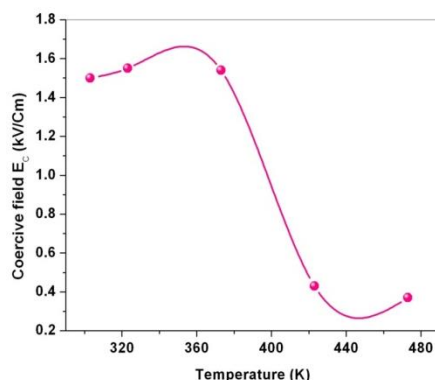


Fig.7 Temperature dependence of coercive field (E_c) of $BaTiO_3$

4. Conclusions

The barium titanate ceramic material is synthesized via conventional solid state reaction method. The cubic structure is confirmed from diffraction study. A high optical band gap of 3.68 eV is attributed to BT when a direct transition is considered. The ferroelectric nature of BT provides a constant saturated polarization of $0.005 \mu\text{C}/\text{cm}^2$. In addition, the coercive field is increased from 1.50-1.55 kV/cm. Further, it is decreased to 0.37 kV/cm.

Acknowledgements

I acknowledge to Dept. of Physics, S.K. University, Anantapur for providing various facilities for sample preparation. Also thankful to Prof. S. Kalainathan, Vellore Institute of Technology (VIT), Tamilnadu for providing P-E loop facility.

References

- [1] K. Chandra Babu Naidu, T. Sofi Sarmash, M. Maddaiah, P. Sreenivasula Reddy, D. Jhansi Rani and T. Subbarao, *Journal of The Australian Ceramic Society* **52**(1), 95 (2016)
- [2] F. Jona, G. Shirane, *Ferroelectric crystals*, Dover Publications, INC., New York, 1993
- [3] K. C. Babu Naidu, T. Sofi Sarmash, M. Maddaiah, A. Gurusampath Kumar, D. Jhansi Rani, V. Sharon Samyuktha, L. Obulapathi, T. Subbarao, *Journal of Ovonic Research* **11**(2), 79 (2015)
- [4] K. Chandra Babu Naidu, T. Sofi Sarmash, V. Narasimha Reddy, M. Maddaiah, P. Sreenivasula Reddy, T. Subbarao, *Journal of The Australian Ceramic Society* **51**(1), 94 (2015).
- [5] K. Chandra Babu Naidu, T. Sofi Sarmash, M. Maddaiah, V. Narasimha Reddy and T. Subbarao, *AIP Conference Proceedings* **1665**, 040001 (2015); doi: 10.1063/1.4917614
- [6] M. Maddaiah, K. Chandra Babu Naidu*, D. Jhansi Rani, T. Subbarao, *Journal of Ovonic Research* **11**(3), 99 (2015)
- [7] S. Prathap, K. Chandra Babu Naidu, and W. Madhuri, *Ferroelectric behaviour of microwave sintered iron deficient $PbFe_{12}O_{19.8}$* , *AIP Conference Proceedings* **1731**, 030019 (2016); doi: 10.1063/1.4947624
- [8] H. Moradmard, S. F. Shayesteh, P. Tohidi, Z. Abbas, M. Khalegi, *Journal of Alloys and Compounds* **650**, 116 (2015).
- [9] Roberto Kofenstein, Till Walther, Dietrich Hesse, Stefan G Ebbinghaus, *Journal of Material Science* **48**, 6509 (2013)
- [10] Wen Fan Chen, Hsin Chen, Pramod Koshy, and Charles Christopher Sorrell, *Journal of The*

Australian Ceramic Society **51**, 1 (2015).

[11]M.A.F.de Souza, R.A.Candeia, A.C.Chaves, S.J.G.Lima, E.Longo, L.E.B.Soledade, I.M.G.Santos, A.G. Souza, Materials Letters **59**, 549 (2005)